A High-Throughput Screen for Porphyrin Metal Chelatases: Application to the Directed Evolution of Ferrochelatases for Metalloporphyrin Biosynthesis

Seok Joon Kwon, Ralf Petri, Arjo L. deBoer, and Claudia Schmidt-Dannert*[a]

Porphyrins are of particular interest in a variety of applications ranging from biocatalysis and chemical synthesis to biosensor and electronic technologies as well as cancer treatment. Recently, we have developed a versatile system for the high-level production of porphyrins in engineered E. coli *cells with the aim of diversifying substitution patterns and accessing porphyrin systems not readily available through chemical synthesis. However, this approach failed to produce significant amounts of the metalloporphyrin in vivo from overproduced protoporphyrin due to insufficient metal insertion. Therefore, we systematically assessed the activity of the* B. subtilis *ferrochelatase in vivo and in vitro. A true high-throughput-screening approach based on catalytic in vivo ferrochelatase activity was developed by using fluorescence-activated cell sorting (FACS). This assay was used to screen a library of 2.4×10^6 ferrochelatase mutants expressed in protoporphyrin-overproducing recombinant* E. coli *cells. Several selected protein variants were purified, and their improved catalytic activity was confirmed in vitro. In addition to ferrochelatase activity, metal transport into E. coli was identified as another limitation for in vivo heme overproduction. Overexpression of the metal transporter* zupT *as part of the assembled pathway increased the overall metalloporphyrin production twofold. This report represents the most exhaustive in vitro evolution study of a ferrochelatase and demonstrates the effectiveness of our novel high-throughput-screening system for directed evolution of ferrochelatases based on their catalytic activity.*

Introduction

Porphyrins are ubiquitous cofactors in nature and play an important role in a variety of essential biological processes, including oxygen storage and transport (myoglobin and hemoglobin), electron transport (cytochromes b and c), and hydrocarbon oxidation (cytochrome P450 and cytochrome oxidase).[1] These proteins bind porphyrins that contain ferrous iron as a central metal ion. Other proteins, like the methyl coenzyme M reductase, contain a hydroporphinoid nickel complex; magnesium is the central metal ion of chlorophylls and bacteriochlorophylls, whereas cobalt is incorporated in the corrin system of vitamin B-12.[2] In addition to their central metal diversity, natural porphyrin systems acquire various substitution patterns and functional groups during their biosynthesis from a common cyclic tetrapyrrole scaffold (uroporphyrinogen III). Their structural and functional variability makes these pigments of considerable interest for numerous applications, such as chemo- and biocatalysis, artificial light-harvesting systems, biological sensors, molecular imprinting, and in cancer research.[3]

So far, these compounds have been chemically synthesized by either total synthesis or functional derivatization of natural metalloporphyrins such as heme.[4] However, biosynthetic-pathway engineering combined with rational and evolutionary protein-design strategies is a promising tool to broaden the accessible structural diversity of tetrapyrrols. We recently developed a versatile system for tailored overproduction of porphyrins in metabolically engineered *Escherichia coli* to serve as starter structures for the applications described above (Scheme 1).[5] However, the overall production of heme in this approach was insufficient even though a ferrochelatase (HemH) was functionally expressed in *E. coli*-overproducing protoporphyrin IX (proto IX); this suggests a limited iron transport into the cell, a low in vivo activity of the ferrochelatase, or both.[5]

Ferrochelatase catalyzes the terminal step in heme biosynthesis, the insertion of Fe^{2+} into proto IX.[6] The most widely adopted catalytic mechanism of the enzyme involves binding of proto IX and the metal ion to the enzyme, distortion of the porphyrin ring to expose the nitrogen lone-pair orbital towards the metal ion, deprotonation of the proto IX, and finally, metal–ligand exchange and release of the heme product.[7]

The catalytic turnover of ferrochelatases is typically low; this indicates a limited ability to differentiate between the porphyrin substrate and the metal-containing product.[8] So far, ferrochelatase activity has not been systematically investigated by in vitro evolution approaches. The major limitation has been the lack of an applicable high-throughput-screening method for the evaluation of large ferrochelatase libraries. Herein, we report the development of such a novel, versatile high-

[a] *Dr. S. J. Kwon, Dr. R. Petri, Dr. A. L. deBoer, Prof. C. Schmidt-Dannert*
Department of Biochemistry, Molecular Biology and Biophysics
University of Minnesota
1479 Gortner Avenue, Saint Paul, MN 55108 (USA)
Fax: (+1) 612-625-5780
E-mail: schmi232@umn.edu

Supporting information for this article is available on the WWW under http://www.chembiochem.org or from the author.

 DOI: 10.1002/cbic.200400051

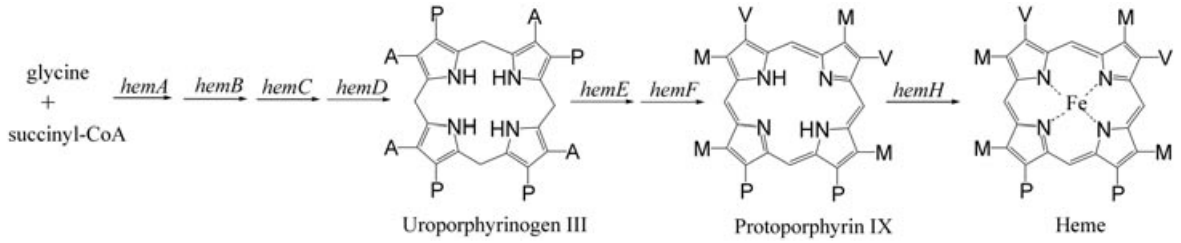

Scheme 1. *Porphyrin synthesis in* E. coli *cells overexpressing heme biosynthetic genes (*hemA–hemH *shown) assembled on three plasmids pAC-*hemABCD*, pBBR-*hemEF*, pUCmod-*hemH.[7] *P: propionate, A: acetate, M: methyl, V: vinyl. The oxidation of protoporphyrinogen to protoporphyrin is either catalyzed by HemF, when the enzyme is overproduced, or occurs spontaneously.*

throughput screening strategy using fluorescence-activated cell sorting (FACS) of ferrochelatase libraries expressed in porphyrin-overproducing *E. coli* cells. Several new ferrochelatase variants with significantly increased iron chelatase activity in vivo and in vitro were obtained.

Results and Discussion

Overexpression of the metal transporter ZupT increases heme biosynthesis

Prior to this study, the entire heme biosynthetic pathway had been assembled by using a three-plasmid system (pAC-*hemABCD*, pBBR-*hemEF*, pUC-*hemH*) and overexpressed in *E. coli*, yielding high levels of porphyrins (up to 90 $\mu mol\,L^{-1}$).[5] However, the insertion of metal into proto IX was inefficient and yielded less then 2 $\mu mol\,L^{-1}$ of heme although the *Bacillus subtilis* ferrochelatase (HemH) was found to be overexpressed and active in vitro.[5] These results indicated either limited iron transport into the cell or the lack of ferrochelatase activity in vivo. In order to investigate a possible metal limitation in vivo, the gene encoding the *E. coli* zinc-uptake protein (ZupT), which belongs to the ZIP (zinc and iron transporter) metal-transporter family and mediates zinc-, iron-, copper-, and cadmium-ion uptake,[9] was cloned and coexpressed in proto IX producing *E. coli* cells containing plasmids pAC-*hemABCD*, pBBR-*hemEF*, and pUC-*hemH* or pUCmod (control). After cultivation of *E. coli* transformants in the presence of $ZnSO_4$ or $FeSO_4$ for 48 h, all porphyrin compounds were extracted and analyzed by HPLC. Overexpression of *zupT* together with the heme pathway doubled the production level of heme and of Zn–proto IX (Table 1 and Figure S1 in the Supporting Information showing HPLC analysis of porphyrin extracts). The same effect was observed when ZupT was overexpressed in proto-IX-producing cells without the *B. subtilis* ferrochelatase (HemH) present in the assembled pathway, probably due to the activity of chromosomal *E. coli* ferrochelatase HemH. These results clearly demonstrated that ZupT was functionally overexpressed as iron and zinc transporter, and indicated that metal uptake is a crucial limitation for overproduction of metal porphyrins in engineered *E. coli*, which can be overcome by metal uptake systems.

Table 1. *Metalloporphyrin biosynthesis in* E. coli *transformants overexpressing the metal-ion transporter ZupT.*

Overexpressed genes[a]	Conversion [%][b]	
	Zn–Proto IX	Heme
hemA, B, C, D, E, F	20.4	7.5
hemA, B, C, D, E, F, H	32.3	12.9
hemA, B, C, D, E, F + zupT	41.1	14.7
hemA, B, C, D, E, F, H + zupT	62.4	21.3

[a] *E. coli* transformants containing three plasmids: pACmod-*hemABCD* and pBBR-*hemEF* or pBBR-*hemEFzupT*, and pUCmod-*hemH* or pUCmod. [b] Calculation of conversion: [metalloporphyrin]/[metalloporphyrin + proto IX] × 100.

Development of a FACS-based high-throughput screen for ferrochelatase activity

Because significant amounts of proto IX still accumulated in cultures overexpressing *zupT*, ferrochelatase activity within the overexpressed heme pathway appeared to be rate limiting (Table 1). To obtain ferrochelatase variants with improved metal-insertion activity in proto IX-overproducing *E. coli* cells, we chose an in vitro evolution approach. Such an approach requires a fast and specific assay for the screening of the large mutant libraries. Unfortunately, reported ferrochelatase in vitro assays are unsuitable for high-throughput screening, as they require anaerobic conditions to maintain the ferrous substrate in the reduced state thus resulting in cumbersome assay procedures and low sensitivities.[10] Alternatively, a stable bivalent zinc ion may substitute the ferrous iron in the assay but the ferrochelatase variants selected for in such a zinc-activity screen may not show the desired enhanced iron-chelatase activity. Thus, a cell-based screen that directly measures in vivo activity by using the natural metal substrate would be the best solution. Since screening for increased heme production in *E. coli* by HPLC analysis is time consuming and laborious, we developed a new high-throughput screening method based on FACS analysis of *E. coli* cells overproducing porphyrins and metalloporphyrins to screen a library of $>10^6$ ferrochelatase variants.

As shown in Figure 1, FACS analysis can efficiently discriminate between three different *E. coli* cell populations at 650 nm (FL3 region): 1) reference cells unable to overproduce porphyrins (containing empty control plasmids pACmod, pBBR1 MCS-2,

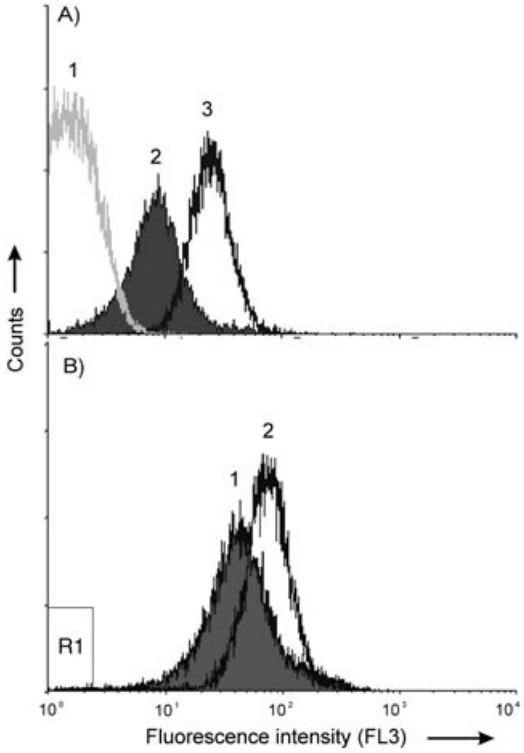

Figure 1. *A) FACS analysis of* E. coli *transformants on the basis of ferrochelatase activity. Control cells (population 1, containing pACmod, pBBR1 MCS-2, pUCmod), Zn–proto IX-producing cells (population 2, containing pAC-*hemABCD, *pBBR-*hemEFzupT, *pUCmod-*hemH168*), and proto IX-producing cells (population 3, containing pAC-*hemABCD, *pBBR-*hemEF, *pUCmod). B) FACS histogram of proto IX-overproducing* E. coli *transformants coexpressing* hemH *wild-type (1) and* hemH *library (2). Region R1 shows the sort gate used to isolate the ferrochelatases with increased activity.*

pUCmod), 2) cells overproducing Zn–proto IX (containing pAC-*hemABCD*, pBBR-*hemEFzupT*, pUCmod-*hemH168*), and 3) cells overproducing proto IX (containing pAC-*hemABCD*, pBBR-*hemEF*, pUCmod). The empty vector reference cells gave only low intensity background fluorescence (population 1, Figure 1 A) whereas the proto IX-overproducing *E. coli* cells gave the highest fluorescence intensity at 650 nm (population 3, Figure 1 A). The insertion of metal into proto IX decreased the fluorescence intensity of the cells as observed with Zn–proto IX-producing *E. coli* cells (population 2, Figure 1 A). Thus, in vivo metalloporphyrin overproduction related to ferrochelatase activity can be detected based on a decrease in proto IX fluorescence intensity, which is independent of the incorporated metal and makes this assay generally applicable for proto IX metal insertion. For convenience of culture handling, preliminary experiments to establish this assay were performed with the stable zinc ion, which offered the additional benefit of direct detection of the produced Zn–proto IX at a blue-shifted emission maximum (578 nm compared to 650 nm for proto IX).

Isolation of ferrochelatase variants with increased chelatase activity

To enhance ferrous iron (Fe^{2+}) activity, the ferrochelatase *hemH* gene from *B. subtilis* 168 was subjected to error-prone PCR, and the resulting mutant library cloned into pUCmod prior to transformation into proto IX-producing *E. coli* cells (containing plasmids pACmod-*hemABCD* and *pBBR-hemEFzupT*). The library was cultivated for 48 h, as described in the Experimental Section, and subsequently sorted by FACS (Figure 1 B). The R1 region of the analyzed population (boxed in Figure 1 B) with the lowest proto IX fluorescence, indicative of a high proto IX-to-heme conversion, was collected. A total of 2.4×10^6 cells were evaluated in 24 min, and 3052 individual clones were recovered and isolated on selective LB agar plates. From these, six clones were picked randomly, cultivated as described, and analyzed by HPLC. The quantitative porphyrin analysis confirmed the increased proto IX-to-heme conversion of the FACS-selected mutants compared to wild-type (WT) HemH (Table 2, Figure 2). Thus, the developed FACS screen for proto IX-producing *E. coli* cells proved to be a powerful and efficient direct high-throughput method for the in vitro evolution of ferrochelatases.

The selected mutant ferrochelatase genes contained one to seven base-pair changes translating into one to three amino acid substitutions (Table 1). To analyze the effects of the mutations in vitro, the ferrochelatase variants and wild-type gene were His-tagged at the C terminus and purified by immobilized metal-affinity chromatography (Figure S2 in the Supporting Information). All mutants, except for mutant M5 (R31G; ca. threefold increase in expression according to SDS-PAGE density data, not shown), were expressed at levels similar to the wild-type gene.

The catalytic properties of the mutants and wild-type ferrochelatase were determined with a discontinuous assay at different Fe^{2+} and proto IX concentrations under anaerobic conditions (to maintain ferrous iron in the reduced state), as reported.[11] The kinetic constants given in Table 2 (V_{max}, k_{cat}, $K_m^{proto\ IX}$, $K_m^{Fe^{II}}$) were calculated from Lineweaver–Burk plots. The detected catalytic turnover rate (k_{cat}) of the wild-type ferro-

Table 2. *Production of heme in recombinant* E. coli *overexpressing the proto IX pathway along with wild-type or mutated* hemH *genes (M1–M6) identified by FACS and catalytic properties of ferrochelatases.*

Ferrochelatases	Conversion[a] [%]	V_{max} [nmol mg^{-1} min^{-1}]	$K_m^{proto\ IX}$ [μM]	$K_m^{Fe^{II}}$ [μM]	k_{cat} [min^{-1}]
Wild-type	44.1	41	0.91	13	1.4
T302A (M1)	74.7	54	0.79	19	1.9
D76G, K102T (M2)	81.9	56	0.44	21	2.0
E61K (M3)	76.1	67	0.78	17	2.4
M11V, G104A (M4)	78.9	65	1.3	9.4	2.3
R31G (M5)	82.4	33	0.83	10	1.2
E61K, L185Q, 212D (M6)	89.3	93	0.86	14	3.3

[a] Calculation of conversion: [heme]/[heme + proto IX]×100.

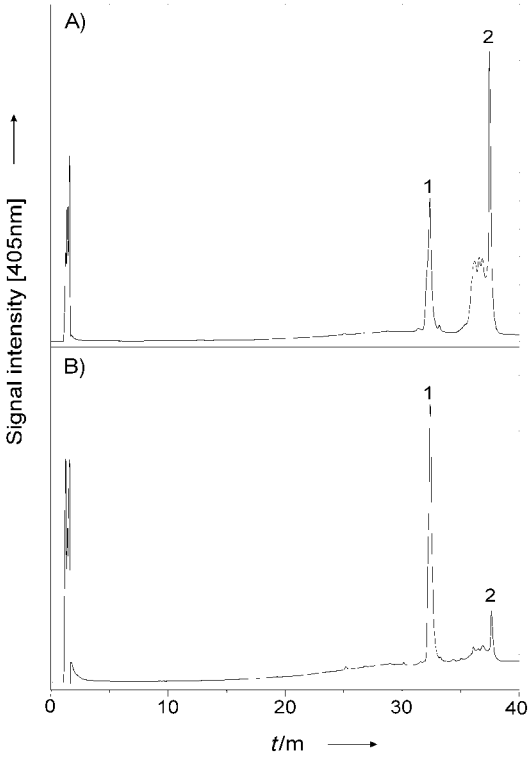

Figure 2. *A) HPLC analysis of porphyrin extracts from* E. coli *transformants harboring A) pAC-*hemABCD, *pBBR-*hemEFzupT, *pUCmod-*hemH *(WT) and B) pAC-*hemABCD, *pBBR-*hemEFzupT, *pUCmod-*hemH *(M6). The separated peaks were identified as heme (peak 1,* λ_{max} *= 502 [*α*], 628 [*β*], and 536 nm [shoulder]; [M+H]*$^+$ *at* m/z *= 616.3) and proto IX (peak 2,* λ_{max} *= 505, 539, 574, and 628 nm; [M+H]*$^+$ *at* m/z *= 563.4).*

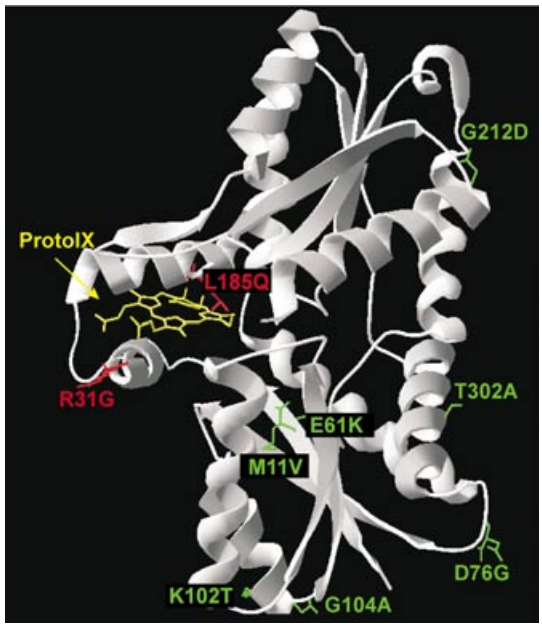

Figure 3. *Structure of the* B. subtilis *ferrochelatase showing the location of the mutations.*

chelatase with iron (Fe^{2+}; 1.4 min^{-1}) was 20-fold lower than that published for Zn^{2+},[11b] this agrees with similar observations described previously,[6] and may be explained by methodological differences between continuous and discontinuous assays as reported by Shi and Ferreira.[10] However, to our knowledge, a direct comparison of Zn^{2+} and Fe^{2+} turnover rates of *B. subtilis* ferrochelatase has not been reported so far. All FACS-selected ferrochelatase mutants, except for the overexpression mutant M5, showed a 1.4–2.4-fold higher catalytic turnover (k_{cat}) compared to the wild-type enzyme.

Structural mapping of ferrochelatase mutations

The obtained mutations were mapped on the X-ray structure of the *B. subtilis* ferrochelatase[12] so as to find explanations for the observed catalytic effects. Except for amino acid substitutions L185Q and R31G, all mutations were located on the surface of the *B. subtilis* protein and far away from the active site (Figure 3).

Interestingly, mutated residue R31 is part of a positively charged "lid", formed by residues R31, R30, R33, and K188, that covers the porphyrin binding cleft and participates in substrate binding.[8] Our data suggest that the loss of a positive charge in mutant R31G (M5) causes the slight decrease of catalytic turnover (k_{cat}) observed. However, the increased expression level over-compensated for the decrease in activity and enhanced heme biosynthesis in vivo (Table 1).

The active site of HemH contains two invariant residues (H183 and E264) and hosts several aromatic residues that limit the space in the porphyrin-binding cleft. From previous calculations it was assumed that ring A of proto IX is tilted 15° out of the plane of the tetrapyrrole, and that the other three rings are tilted as well: ring C is slightly tilted, about 4°, in the same direction, whereas rings B and D are tilted in the opposite direction, by 2° and 9°, respectively.[6b] The authors suggested that the saddled structure of the tilted proto IX facilitates the insertion of the central metal ion into the tetrapyrrole. These data were later partially confirmed by the X-ray structure, which disclosed that the invariant glutamate residue E264 was responsible for the distortion of ring A. The residue L185, discovered from mutant M6 (E61K, L185Q, G212D), is one of the few nonaromatic residues in the active site, is located above the pyrrole rings B and C of the tetrapyrrole (Figure 3), and may alter distortion of the tetrapyrrole ring upon substitution. If so, this particular residue may be a hotspot for increasing ferrochelatase activities by using rational design strategies. Further investigation into this is currently underway.

Conclusion

Intriguingly, most of the mutations selected by FACS analysis were located on the surface of the protein. As the *B. subtilis* ferrochelatase is soluble, it differs from most other ferrochelatases, which are membrane-associated.[11,13] Our mutants, with increased in vivo activity based on certain structural or electrostatic changes at the surface of the *B. subtilis* ferrochelatase (Figure 3, Table 1), might therefore reflect a membrane or protein–protein interaction, which possibly enhances activity.

However, our in vitro data confirmed that all mutants have enhanced catalytic turnover rates (Table 2); this suggests a combination of surface effects and long-range activity effects.

This report represents the most exhaustive in vitro evolution approach to ferrochelatases and successfully combines assay development with directed-evolution methods and in vivo production of porphyrin compounds. We have demonstrated the effectiveness and power of our novel high-throughput-screening system for the directed evolution of ferrochelatase genes based on catalytic activity. The results presented herein enable us to discover new ferrochelatase variants with higher activity by rational and in vitro evolutionary approaches.

Experimental Section

Bacterial strains, plasmids, and cultivation: Strains and plasmids used in this study are listed in Table S1 in the Supporting Information. The proto IX pathway consisting of genes *hemA*, *hemB*, *hemC*, *hemD*, *hemE*, and *hemF* was cloned in a modular fashion on plasmids pACmod and pBRR1MCS-2 yielding plasmids pAC-*hemABCD*, pBBR-*hemEF* as reported.[5] *B. subtilis* ferrochelatase *hemH* was cloned on pUCmod.[14] *E. coli* were routinely grown in LB medium supplemented with carbenicillin (100 $\mu g\,mL^{-1}$), chloramphenicol (50 $\mu g\,mL^{-1}$), and kanamycin (30 $\mu g\,mL^{-1}$) where appropriate.

The *zupT* gene from *E. coli* (GenBank Accession No.: AE000386)[9] was amplified from chromosomal DNA and cloned into the pUCmod. The cloned gene (*zupT*), including the *lac*-promoter, was reamplified from pUC-*zupT* and assembled into pBBR1-*hemEF* yielding pBBR-*hemEFzupT*. For purification purposes, a modified vector pUC-His was constructed from pUCmod following a QuickChange™ protocol (Stratagene, CA) by using the primers pUChis-F (5′-GACTCGAGCATCACCATCACCATCACTGATTCTCCTTACGCATCTGTG-CG-3′) and pUChis-R (5′-TCAGTGATGGTGATGGTGATGCTCGAGCG-GAATACCGCAGCGGCCGC-3′), creating a new *Xho*I-site for subsequent cloning in frame with the His-tag.

Analysis of metalloporphyrins: *E. coli* transformants were grown for 24 h at 30 °C in selective LB medium (50 mL). After 24 h, $ZnSO_4$ (100 μM) or $FeSO_4$ (500 μM) was added into the media, and the bacterial cells were cultivated aerobically another 24 h for direct comparison of Fe and Zn uptake. The cells were harvested by centrifugation (4000 *g*, 20 min), resuspended in Tris/HCl (100 mM, pH 7.6) containing EDTA (50 mM) to remove the divalent ions added, washed twice with Tris/HCl (pH 7.6), and finally extracted with acetone/6 N hydrochloric acid (10:1). HPLC and LC-MS analysis were performed as described.[5]

Library construction and FACS analysis: The initial library of ferrochelatase mutants was created by error-prone PCR of the *hemH* gene from *B. subtilis* by using the Diversify™ PCR Random Mutagenesis Kit (Becton Dickinson, San Jose, CA). The amplification products were ligated into pUCmod,[14] pooled, and transformed into proto IX-producing *E. coli*[5] containing pACmod-*hemABCD* and pBBR-*hemEFzupT* for library screening. The transformants were cultivated for 24 h at 30 °C in LB media (50 mL) containing carbenicillin (100 $\mu g\,mL^{-1}$), chloramphenicol (50 $\mu g\,mL^{-1}$), and kanamycin (30 $\mu g\,mL^{-1}$). After 24 h, $FeSO_4$ (500 μM) was added to the media, and the bacterial cells were incubated anaerobically (to reduce iron oxidation) for another 24 h. An aliquot (100 μL) of culture was pelleted, and the cells were washed three times with PBS buffer (1 mL), suspended in PBS buffer (1 mL), and examined with the FACSCalibur™ Flow Cytometry System (Becton Dickinson, Oxnard, CA). Empty plasmids and wild-type ferrochelatase were used as controls. Sorting was performed in exclusion mode on about 10^6 events at approximately 2000 events per second. After sorting, the cells were isolated on LB plates containing carbenicillin (100 $\mu g\,mL^{-1}$), chloramphenicol (50 $\mu g\,mL^{-1}$), and kanamycin (30 $\mu g\,mL^{-1}$) at 30 °C for 24 h. The clones for further in vitro experiments were randomly picked from the plate and cultivated in LB media (50 mL) as described above.

Enzyme purification and kinetic analysis: His-tagged ferrochelatases (wild-type and variants) were purified by using metal-affinity chromatography (BD Talon™, San Jose, CA). Protein purity was assessed by SDS-PAGE, and protein concentrations were determined by using the Bio-Rad protein assay (Hercules, CA) with bovine serum albumin as standard. Ferrochelatase activity was assayed by measuring the rate of proto IX disappearance[15] (excitation at 410 nm and emission at 634 nm) with a Gemini XS spectrofluorometer from Molecular Device (Sunnyvale, CA). The reaction mixture (1 mL) contained proto IX (0.75, 1.5, 2.5 μM) and 10 μg of purified ferrochelatases (wild-type and variants) in Tris/HCl (100 mM, pH 7.6) and Tween 80 (0.5% *v/v*) at 30 °C. The reaction was initiated by injecting ferrous iron (12.5, 25, 50 μM). Anaerobic conditions were maintained in septum-capped reaction vials by a continuous nitrogen stream to keep iron in its reduced ferrous state.

Structure analysis. The mutations were identified in the X-ray structure of *Bacillus subtilis* HemH (PDB database entry 1C1H) by using SWISS-PDB software.[16]

Acknowledgements

This research was supported by the National Institutes of Health (grant NIH/1R01-GM65471-01) and by the David and Lucile Packard Foundation (grant 2001-18996).

Keywords: ferrochelatase · fluorescence-activated cell sorting · high-throughput screening · iron · porphyrins

[1] a) D. A. Mills, S. Ferguson-Miller, *FEBS Lett.* **2003**, *545*, 47; b) S. Adachi, S. Y. Park, J. R. Tame, Y. Shiro, N. Shibayama, *Proc. Natl. Acad. Sci. USA* **2003**, *100*, 7039; c) S. Kundu, S. A. Premer, J. A. Hoy, J. T. Trent III, M. S. Hargrove, *Biophys. J.* **2003**, *84*, 3931; d) V. Guallar, M. H. Baik, S. J. Lippard, R. A. Friesner, *Proc. Natl. Acad. Sci. USA* **2003**, *100*, 6998; e) S. Shaik, S. P. de Visser, F. Ogliaro, H. Schwarz, D. Schroeder, *Curr. Opin. Chem. Biol.* **2002**, *6*, 556.

[2] a) U. Ermler, W. Grabarse, S. Shima, M. Goubeaud, R. K. Thauer, *Science* **1997**, *278*, 1457; b) A. Strand, T. Asami, J. Alonso, J. R. Ecker, J. Chory, *Nature* **2003**, *421*, 79; c) J. H. Martens, H. Barg, M. J. Warren, D. Jahn, *Appl. Microbiol. Biotechnol.* **2002**, *58*, 275; d) A. R. Battersby, *Nat. Prod. Rep.* **2000**, *17*, 507.

[3] a) P. Thordarson, E. J. Bijsterveld, A. E. Rowan, R. J. Nolte, *Nature* **2003**, *424*, 915; b) M. Andersson, M. Linke, J. C. Chambron, J. Davidsson, V. Heitz, L. Hammarstrom, J. P. Sauvage, *J. Am. Chem. Soc.* **2002**, *124*, 4347; c) N. A. Rakow, K. S. Suslick, *Nature* **2000**, *406*, 710; d) A. Tsuda, A. Osuka, *Science* **2001**, *293*, 79; e) N. Aratani, H. S. Cho, T. K. Ahn, S. Cho, D. Kim, H. Sumi, A. Osuka, *J. Am. Chem. Soc.* **2003**, *125*, 9668; f) T. W. Wong, E. Tracy, A. R. Oseroff, H. Baumann, *Cancer Res.* **2003**, *63*, 3812; g) S. C. Zimmerman, M. S. Wendland, N. A. Rakow, I. Zharov, K. S. Suslick, *Nature* **2002**, *418*, 399; h) Z. M. Liu, A. A. Yasseri, J. S. Lindsey, D. F. Bocian, *Science* **2003**, *302*, 1543.

[4] *The Porphyrin Handbook, Vol. 1–10* (Eds.: K. M. Kadish, K. M. Smith, R. Guilard), Academic Press, San Diego, **2000**.

[5] S. J. Kwon, A. L. de Boer, R. Petri, C. Schmidt-Dannert, *Appl. Environ. Microbiol.* **2003**, *69*, 4875.

[6] a) H. A. Dailey, *J. Biol. Inorg. Chem.* **1997**, *2*, 411; b) D. Lecerof, M. Fodje, A. Hansson, M. Hansson, S. Al-Karadaghi, *J. Mol. Biol.* **2000**, *297*, 221.
[7] a) H. A. Dailey, J. E. Fleming, *J. Biol. Chem.* **1983**, *258*, 11 453; b) E. Sigfridsson, U. Ryde, *J. Biol. Inorg. Chem.* **2003**, *8*, 273.
[8] H. A. Dailey, T. A. Dailey, C. K. Wu, A. E. Medlock, K. F. Wang, J. P. Rose, B. C. Wang, *Cell. Mol. Life Sci.* **2000**, *57*, 1909.
[9] a) G. Grass, M. D. Wong, B. P. Rosen, R. L. Smith, C. Rensing, *J. Bacteriol.* **2002**, *184*, 864; b) M. L. Guerinot, *Biochim. Biophys. Acta* **2000**, *1465*, 190.
[10] Z. Shi, G. C. Ferreira, *Anal. Biochem.* **2003**, *318*, 18.
[11] a) M. Hansson, L. Hederstedt, *Eur. J. Biochem.* **1994**, *220*, 201; b) U. Olsson, A. Billberg, S. Sjövall, S. Al-Karadaghi, M. Hansson, *J. Bacteriol.* **2002**, *184*, 4018.
[12] S. Al-Karadaghi, M. Hansson, S. Nikonov, B. Jonsson, L. Hederstedt, *Structure* **1997**, *5*, 1501.
[13] K. F. Wang, T. A. Dailey, H. A. Dailey, *FEMS Microbiol. Lett.* **2001**, *202*, 115.
[14] C. Schmidt-Dannert, *Biochemistry* **2001**, *40*, 13 125.
[15] J. M. Camadro, P. Labbe, *J. Biol. Chem.* **1988**, *263*, 11 675.
[16] T. Schwede, J. Kopp, N. Guex, M. C. Peitsch, *Nucleic Acids Res.* **2003**, *31*, 3381.

Received: February 20, 2004

